Sandwiched Graphene–Membrane Superstructures

Alexey V. Titov, Petr Král,* and Ryan Pearson

Department of Chemistry, University of Illinois at Chicago, Chicago, Illinois 60607

ARTICLE

ABSTRACT We demonstrate by molecular dynamics simulations that graphene sheets could be hosted in the hydrophobic interior of biological membranes formed by amphiphilic phospholipid molecules. Our simulation shows that these hybrid graphene–membrane superstructures might be prepared by forming hydrated micelles of individual graphene flakes covered by phospholipids, which can be then fused with the membrane. Since the phospholipid layers of the membrane electrically isolate the embedded graphene from the external solution, the composite system might be used in the development of biosensors and bioelectronic materials.

KEYWORDS: graphene · lipid membrane · self-assembly · graphene composite · bioelectronics

Recently discovered graphene monolayers with superb material properties could yield unprecedented applications,[1] such as graphene-based electronic nanodevices.[2−4] The atomically thin graphene monolayers have very high strength and rigidity, due to covalent binding of carbon atoms *via* planar sp^2-orbitals.[5] Their semi-metallic electrical conductivity is provided by massless Dirac electrons in hybridized unsaturated π_z molecular orbitals.[6] Electronic properties of graphene can be tuned by doping[7,8] and chemical functionalization.[9,10] It would be particularly attractive to stabilize graphene-based electronic materials directly inside biological cells.[11]

Although graphene is not soluble in polar solvents, it forms stable dispersions in organic solvents upon chemical functionalization.[12] Carbon nanotubes (CNT)[13,14] and fullerenes[15] form stable assemblies with lipid bilayers in cellular membranes, composed of layered 1-palmitoyl-2-oleoyl-*sn*-glycero-3-phosphocholine phospholipids (POPC). Planar graphene monolayers could provide better hybridization with the two-dimensional cellular membranes. Potentially, these graphene layers, electrically isolated by the POPC layers from physiological solutions inside the cells, could be electronically activated and connected with other biological structures.

In this work, we use molecular dynamics (MD) simulations to test if these superstructures could be formed. Since the self-assembly of such composite systems can take hundreds of nanoseconds,[16,17] we resort to coarse-grained molecular dynamics (CGMD) simulations.[18−20] We use the Martini 2.0 force field,[21] implemented in the NAMD package.[22−24] Coarse graining of the POPC molecules is performed through a four-to-one atom-mapping procedure,[18] where every four non-hydrogen atoms in the lipids are modeled as a single bead. The amine and phosphate head groups of POPC are represented by the Qo- and Qa-type beads, respectively.[21] The coarse-grained (CG) hydrophobic tails are represented by the C1-type beads.[21] Similarly, every four water molecules are united into a single P4-type bead. The honeycomb structure of graphene is reduced to a triangular lattice of CG beads, where every three carbons in the all-atom graphene are modeled as a SC4-type bead and the nonbonded interactions between the beads are defined in the Martini 2.0 force field (see Simulation Details).[21]

Parametrization of the nonbonded interactions is important for a proper description of this hybrid system, characterized by the interplay between the lipid–lipid and lipid–graphene interactions. Recent experiments have demonstrated that noncovalent adsorption of amphiphiles on CNTs preserves the electronic structure of the tubes and provides their superior solubility.[13,25−27] CGMD modeling of the self-assembly of detergents and lipids on CNTs[19,20] can be well matched to these experiments.[13,27] We use the same approach, but the aromatic

*Address correspondence to pkral@uic.edu.

Received for review November 6, 2009 and accepted December 14, 2009.

Published online December 21, 2009.
10.1021/nn9015778

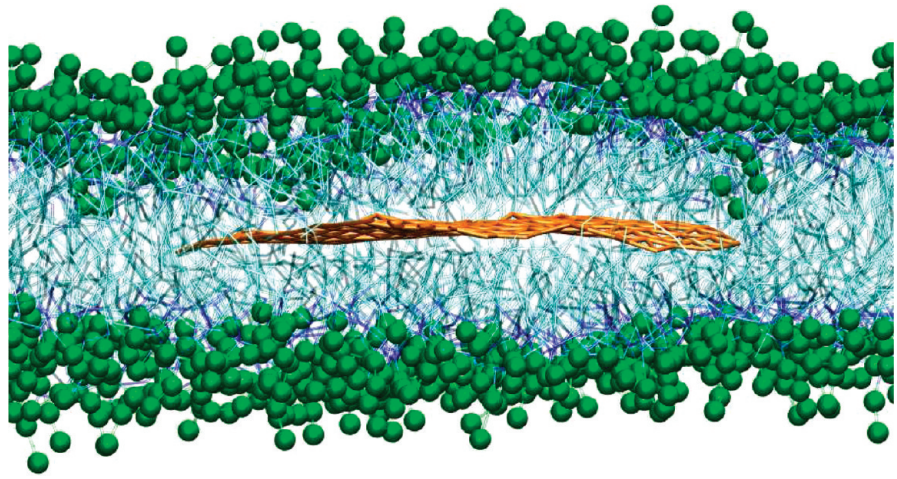

Figure 1. Equilibrated superstructure of graphene sheet hosted inside the phospholipid bilayer membrane formed by POPC lipids. Polar heads of the POPC lipids are shown with green beads, hydrophobic hydrocarbon chains and the graphene sheet are shown with thick blue and brown lines, respectively (water beads hidden).

carbons of graphene are approximated slightly differently. The area per CG carbon particle equals ≈13.49 and ≈11.42 Å in our and the latter models, respectively. Instead of a simple "hydrophobic apolar" bead C, we use a SC4-type bead, which describes benzene molecules in the Marrink's force field.[21] In this way, the graphene−lipid tail interaction per bead is 14% smaller than the lipid−lipid tail interaction, but the average area per CG carbon in our graphene model is 18% larger than in the CG CNT.[19] The robustness of this approach has been verified earlier by varying CNT−lipid interaction while keeping the lipid−lipid interaction the same.[19]

RESULTS AND DISCUSSION

Once we establish the model parameters, we simulate equilibration of the CG graphene monolayer inside the CG bilayer membrane. In Figure 1, we show the rectangular graphene sheet (size of ≈5.9 × 6.2 nm^2) with 271 SC4-type beads equilibrated inside the bilayer membrane, formed by 637 POPC lipids. The composite system is modeled as an NPT ensemble, with periodic boundary conditions applied, the pressure of $P = 1$ atm and temperature of $T = 310$ K. We use the Langevin Piston method,[28] where the Langevin damping coefficient is 1 ps^{-1} and the simulation time step is $t = 8$ fs. The membrane is kept under zero lateral tension, which reproduces well the experimentally observed density of POPC lipids of 1 lipid per 0.65 nm^2.[29] The graphene monolayer is initially placed between the two membrane layers, and the system is equilibrated for $\tau > 100$ ns. The simulations show that the thickness of the lipid bilayer is almost not affected by the incorporation of the graphene monolayer. Over the time, the graphene monolayer slowly diffuses in the membrane interior, but the composite system stays stable.

Next, we investigate how the graphene monolayers could be inserted inside the bilayer membranes and potentially stabilized to form the composite systems. We first prepare a micelle formed by the above graphene monolayer covered from both sides by 91 POPC lipids. The micelle is equilibrated and placed close to the membrane, as shown in Figure 2a. As the micelle slowly merges with the top lipid layer, some lipids become trapped below the attached micelle (Figure 2b). At $t \approx$ 100−120 ns, the lipids that belonged to the micelle start to form a neck-like protrusion to the bottom part of the bilayer (Figure 2c). This initiates fusion of the graphene into the membrane at $t \approx$ 300−360 ns when the graphene monolayer starts to enter the interior of the lipid bilayer in an energetically favorable tilted fashion, as shown in Figure 2d,e. This process progresses until the graphene is stabilized in the center of the bilayer membrane at $t \approx$ 516 ns (Figure 2f). We expect that the graphene self-insertion should be faster at higher temperatures, but the process might take longer for larger sheets (experimentally available).

Once the composite system becomes locally stabilized, at Figure 2f, an *unequal* number of lipids would stay on both sides of the membrane. This is because the once-trapped lipids remain predominantly at the top layer of the membrane. In natural systems, phospholipids diffuse relatively fast on each side of the membrane. They are also randomly transferred with the rate of 10^{-5} s from one side of the membrane to the other side by flippase and floppase proteins.[30,31] In our small simulation cell, we model the transversal equilibration of the POPC lipids by pulling every 2 ns a randomly chosen lipid from one side of the membrane to the other.

It is important to estimate the stability of the composite systems formed. Here, we calculate the work invested into removing the equilibrated graphene monolayer from the membrane. We pull the monolayer (≈5.9 × 6.2 nm^2) out of the membrane (≈13.5 × 13.5 nm^2)

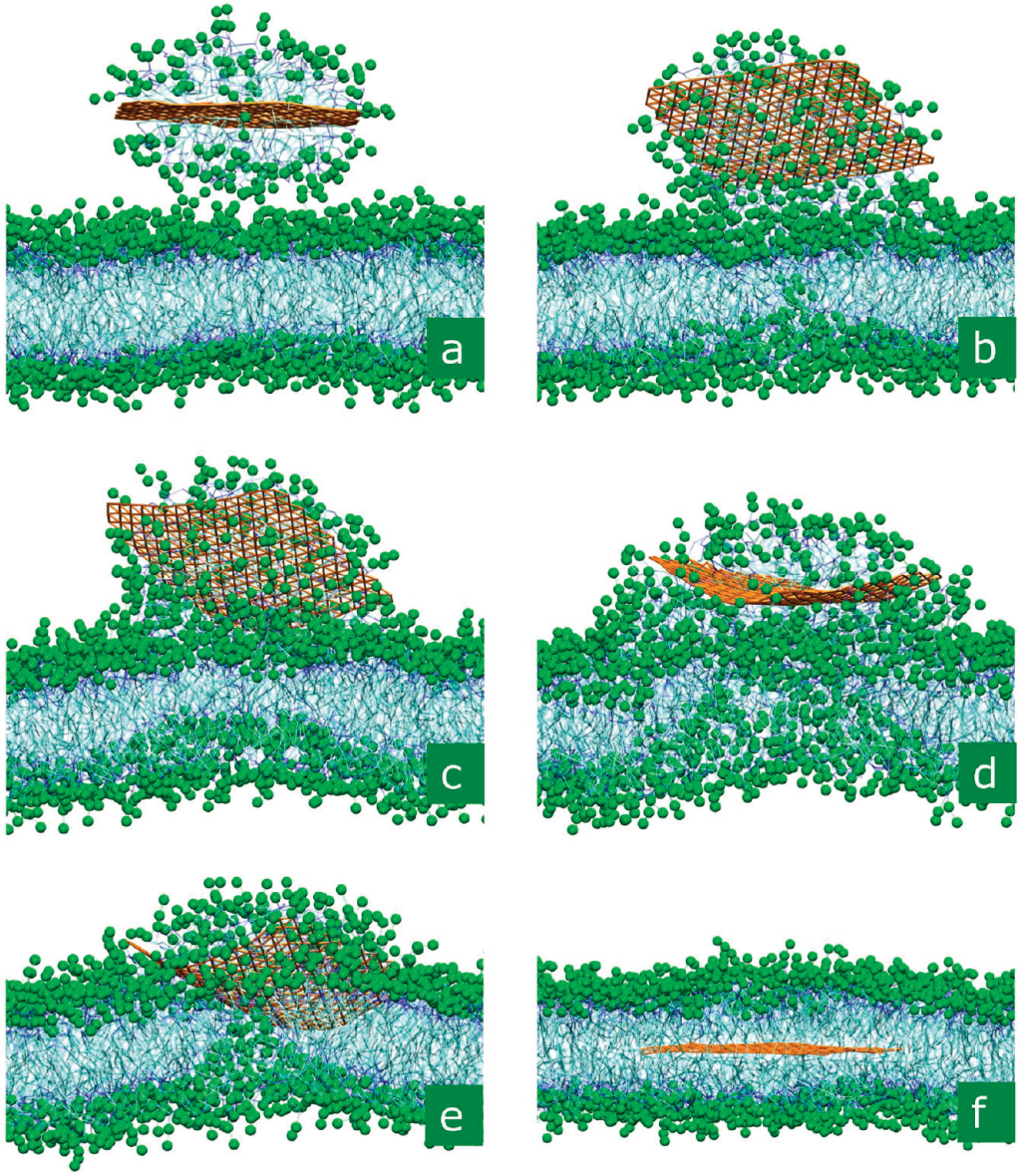

Figure 2. Self-insertion of graphene monolayer inside the phospholipid membrane. In the displayed process, a graphene micelle merges with the membrane and releases the monolayer, which penetrates the membrane. The snapshots are taken at t_{a-f} = 2.9, 52.4, 120.0, 299.2, 356.4, and 516.4 ns, respectively.

composed of 546 POPC lipids. During the simulations, we spatially fix 26 polar heads of POPC lipids on the edges of the bottom phospholipid layer, in order to keep the membrane in place. In Figure 3, we plot the equilibrium vertical displacement of the graphene edge to which a static vertical force F is applied. The dependence is monotonous, but at $F = 0.17$ nN, we can see a small nonlinearity in the displacement caused by rupturing of the top layer in the membrane (thin vertical line in Figure 3). At larger forces, the dependence of h on F is practically linear.

By integrating the force and the differential displacement, we can calculate the approximate binding energy of the graphene to the membrane

$$\Delta E(h_{max}) = \int_0^{h_{max}} F(h)dh \qquad (1)$$

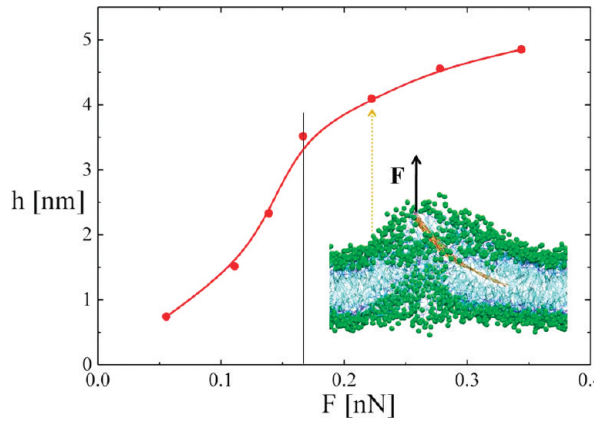

Figure 3. Dependence of the equilibrium elevation of the graphene sheet (≈5.9 × 6.2 nm^2) above the membrane (546 lipids) upon application of a static vertical force F. (Inset) Snapshot of the equilibrated structure for total force F = 0.22 nN.

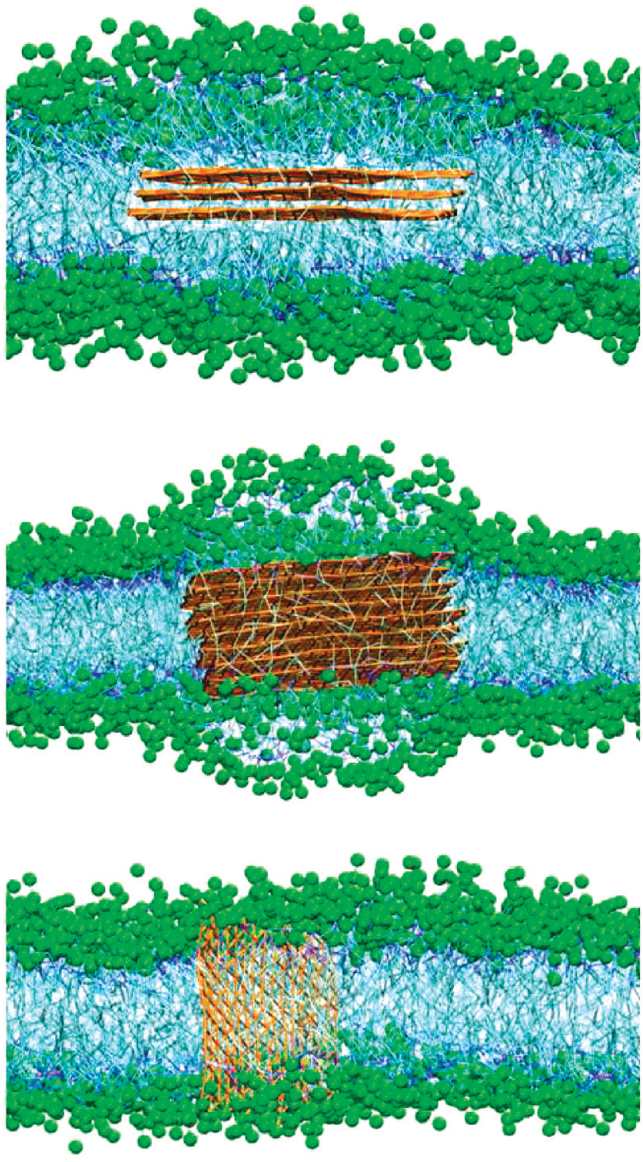

Figure 4. (Top to bottom) Equilibrated composite structures with three and eight graphene monolayers (≈5.9 × 6.2 nm^2), as well as a vertically oriented graphene sheet (≈4.3 × 5.9 nm^2), with two-edge functionalizations by the polar heads of POPC lipids, all stabilized inside the POPC bilayer membrane.

Here, h_{max} is the final displacement of the graphene, which depends on the total force F applied to it. From eq 1, we obtain the graphene binding (extraction) energy of $\Delta E \approx 41.7$ kcal/mol (66.9 kT) if we slowly increase the total force from $F = 0$ to the chosen maximum value of $F_{max} = 0.35$ nN. In the linear regime, we can obtain the graphene binding energies of $\Delta E \approx 1.13$ kcal/mol per nm^2. These values confirm that graphene monolayers can be stabilized in the hydrophobic interior of the bilayer membrane at room temperature.

Finally, we briefly investigate if other composite systems can be formed. First, we study superstructures with several stacked graphene monolayers incorporated inside the bilayer membrane, as displayed in Figure 4. The equilibrium thickness of the lipid bilayer of $w_m \approx 4.3$ nm changes on average by $\Delta w_m \approx 0.9$ and 2.6 nm in the case of three- and eight-stacked graphene monolayers hosted in the membrane, respectively. We also test if graphene stripes can be hosted vertically in the membrane. This could, for example, serve the purpose of controlling molecular traffic in the membrane. We pick a graphene stripe (≈4.3 × 5.9 nm^2) of a width similar to the membrane thickness ($w_m \approx 4.3$ nm). Two of its opposite sides are functionalized by polar ligands of the same type as used in the POPC lipids. The equilibrated composite superstructure is shown in the bottom of Figure 4. Although we have not tested the self-insertion of all these structures, we believe that they can be spontaneously stabilized as in Figure 2f, due to minimization of their Gibbs energies.

Our computational study of lipid bilayer is limited to a small number of components. These results would be mostly valid on pure phospholipid membranes prepared *in vitro*. The graphene encapsulation into multicomponent cellular membranes *in vivo*, with its complex nature and uncertainty in structure of lipid bilayer,[32,33] would need further investigation. The insertion might be hindered by membrane trafficking processes, changes in the lipid composition, the presence of cholesterol molecules, and various membrane proteins.[34−38]

CONCLUSIONS

In summary, we have introduced composite systems formed by graphene monolayers sandwiched inside phospholipid membranes. These unique superstructures could serve as a platform for graphene-based nanomaterials integrated inside biological membranes. Several examples demonstrating bioconjugation with graphene have been recently reported. The combination of graphene with biocomponents at the micrometer scale has allowed the preparation of a single bacteria graphene sensor and a DNA transistor.[39] Biosensing of glucose on graphene and specific CNT binding to α-chymotrypsin, regulating its enzymatic activity, have also been demonstrated.[40,41] Analogously, electronic circuits might potentially be made when graphene is integrated into biological membranes since the phospholipid molecules could isolate the embedded graphene layers from the electrically conducting physiological solutions present inside biological systems. Similarly to CNT−lipid assemblies,[13,14,20] such composite systems could be used for the development of biosensors and bioelectronic nanomaterials. With the wider availability of graphene, the verification of our findings should be straightforward, and the discussed exciting possibilities might be experimentally realized in the near future.[42]

SIMULATION DETAILS

The graphene is modeled with a triangular lattice of the SC4-type beads, where the angular force constants and equilibrium angles are given by $K_{angle} = 700$ kcal mol^{-1} rad^{-2} and $\theta_0 = 60°$, respectively. The dihedral angle force constants, multiplicity, and potential minima are defined as $K_\chi = 3.1$ kcal mol^{-1}, $n = 2$, and $\delta = 180°$, respectively. Our CGMD simulation time flows about four times faster than the all-atom MD simulation time.[18]

Proper modeling of the graphene elasticity is important for the consistency of the CGMD simulations, even though graphene sheets inside the lipid bilayers are not likely to be subjected to large stretching deformations. We calibrate the Young's modulus in our CGMD model to the experimentally found elasticity of graphene. Experiments on bulk graphite give ≈1 TPa for the in-plane Young's modulus,[43] while the Young's modulus in graphene varies between 0.5 and 1.0 TPa.[44,45]

To compare Young's modulus with the macroscopic values, we keep one edge of the graphene sheet (≈5.9 × 6.2 nm^2) fixed and apply a constant force to the opposite edge. The normal stress is found as

$$\sigma = \frac{nF}{w_g t_g} \tag{2}$$

where n is the number of CG beads with applied tensile force F, w_g is the width and t_g is the thickness of the graphene (separation of graphene layers in graphite), respectively. In classical mechanics the Young's modulus is defined as

$$E = \frac{\sigma}{\Delta l / l} \tag{3}$$

where l and Δl are the equilibrium length of the graphene sheet and its change with the applied force, respectively. Our initial all-atom model of graphene yields its Young's modulus of $E \approx 0.9$ TPa, where the used bond and angular constants are 322.5 kcal mol^{-1} Å^{-2} and 53.35 kcal mol^{-1} rad^{-2}, respectively. We have realized that, in order to have a similar Young's modulus in the CGMD model, we need to adjust these constants to 700 kcal mol^{-1} Å^{-2} and 700 kcal mol^{-1} rad^{-2}, respectively. When we stretch this system in simulations and use eqs 2 and 3, we obtain $E_{CGMD} = 928$ GPa for the graphene sheet with $n = 9$, $w_g = 5.9$ nm, $t_g = 0.34$ nm, $F = 69.47$ pN, and $\Delta l / l = 0.00034$. However, the stiffness of the model graphene is less important for the behavior of the described composite planar systems, as confirmed in our modeling.

Acknowledgment. We acknowledge Aleksei Aksimentiev and Rogan Carr for discussions of the CG simulations. A.T. acknowledges the UIC Office of Research for support.

Supporting Information Available: Video of graphene insertion into the POPC bilayer. This material is available free of charge *via* the Internet at http://pubs.acs.org.

REFERENCES AND NOTES

1. Novoselov, K. S.; Geim, A. K.; Morozov, S. V.; Jiang, D.; Katsnelson, M. I.; Grigorieva, I. V.; Dubonos, S. V.; Firsov, A. A. Two-Dimensional Gas of Massless Dirac Fermions in Graphene. *Nature* **2005**, *438*, 197–200.
2. Miao, F.; Wijeratne, S.; Zhang, Y.; Coskun, U. C.; Bao, W.; Lau, C. N. Phase-Coherent Transport in Graphene Quantum Billiards. *Science* **2007**, *317*, 1530–1533.
3. Castro, E. V.; Novoselov, K. S.; Morozov, S. V.; Peres, N. M. R.; Dos Santos, J. M. B. L.; Nilsson, J.; Guinea, F.; Geim, A. K.; Neto, A. H. C. Biased Bilayer Graphene: Semiconductor with a Gap Tunable by the Electric Field Effect. *Phys. Rev. Lett.* **2007**, *99*, 216802.
4. Ponomarenko, L. A.; Schedin, F.; Katsnelson, M. I.; Yang, R.; Hill, E. W.; Novoselov, K. S.; Geim, A. K. Chaotic Dirac Billiard in Graphene Quantum Dots. *Science* **2008**, *320*, 356–358.
5. Saito, R.; Fujita, M.; Dresselhaus, G.; Dresselhaus, M. S. Electronic Structure of Chiral Graphene Tubules. *Appl. Phys. Lett.* **1992**, *60*, 2204–2206.
6. Avouris, P.; Chen, Z. H.; Perebeinos, V. Carbon-Based Electronics. *Nat. Nano* **2007**, *2*, 605–615.
7. Stankovich, S.; Dikin, D. A.; Dommett, G. H. B.; Kohlhaas, K. M.; Zimney, E. J.; Stach, E. A.; Piner, R. D.; Nguyen, S. T.; Ruoff, R. S. Graphene-Based Composite Materials. *Nature* **2006**, *442*, 282–286.
8. Dikin, D. A.; Stankovich, S.; Zimney, E. J.; Piner, R. D.; Dommett, G. H. B.; Evmenenko, G.; Nguyen, S. T.; Ruoff, R. S. Preparation and Characterization of Graphene Oxide Paper. *Nature* **2007**, *448*, 457–460.
9. Cervantes-Sodi, F.; Csanyi, G.; Piscanec, S.; Ferrari, A. C. Edge-Functionalized and Substitutionally Doped Graphene Nanoribbons: Electronic and Spin Properties. *Phys. Rev. B* **2008**, *77*, 165427.
10. Boukhvalov, D. W.; Katsnelson, M. I. Chemical Functionalization of Graphene with Defects. *Nano Lett.* **2008**, *8*, 4373–4379.
11. Král, P. Control of Catalytic Activity of Proteins *In Vivo* by Nanotube Ropes Excited with Infrared Light. *Chem. Phys. Lett.* **2003**, *382*, 399–403.
12. Konatham, D.; Striolo, A. Molecular Design of Stable Graphene Nanosheets Dispersions. *Nano Lett.* **2008**, *8*, 4630–4641.
13. Richard, C.; Balavoine, F.; Schultz, P.; Ebbesen, T. W.; Mioskowski, C. Supramolecular Self-Assembly of Lipid Derivatives on Carbon Nanotubes. *Science* **2003**, *300*, 775–778.
14. Thauvin, C.; Rickling, S.; Schultz, P.; Celia, H.; Meunier, S.; Mioskowski, C. Carbon Nanotubes as Templates for Polymerized Lipid Assemblies. *Nat. Nano* **2008**, *3*, 743–748.
15. Wong-Ekkabut, J.; Baoukina, S.; Triampo, W.; Tang, I.-M.; Tieleman, D. P.; Monticelli, L. Computer Simulation Study of Fullerene Translocation through Lipid Membranes. *Nat. Nano* **2008**, *3*, 363–368.
16. Carr, R.; Weinstock, I. A.; Sivaprasadarao, A.; Muller, A.; Aksimentiev, A. Synthetic Ion Channels *via* Self-Assembly: A Route for Embedding Porous Polyoxometalate Nanocapsules in Lipid Bilayer Membranes. *Nano Lett.* **2008**, *8*, 3916–3921.
17. Neri, M.; Baaden, M.; Carnevale, V.; Anselmi, C.; Maritan, A.; Carloni, P. Microseconds Dynamics Simulations of the Outer-Membrane Protease T. *Biophys. J.* **2008**, *94*, 71–78.
18. Marrink, S.; deVries, A.; Mark, A. Coarse Grained Model for Semiquantitative Lipid Simulations. *J. Phys. Chem. B* **2004**, *108*, 750–760.
19. Wallace, E. J.; Sansom, M. S. P. Carbon Nanotube/Detergent Interactions *via* Coarse-Grained Molecular Dynamics. *Nano Lett.* **2007**, *7*, 1923–1928.
20. Wallace, E. J.; Sansom, M. S. P. Carbon Nanotube Self-Assembly with Lipids and Detergent: A Molecular Dynamics Study. *Nanotechnology* **2009**, *20*, 045101.
21. Marrink, S. J.; Risselada, H. J.; Yefimov, S.; Tieleman, D. P.; de Vries, A. H. The MARTINI Force Field: Coarse Grained Model for Biomolecular Simulations. *J. Phys. Chem. B* **2007**, *111*, 7812–7824.
22. Phillips, J. C.; Braun, R.; Wang, W.; Gumbart, J.; Tajkhorshid, E.; Villa, E.; Chipot, C.; Skeel, R. D.; Kale, L.; Schulten, K.; Schulten, K. Scalable Molecular Dynamics with NAMD. *J. Comput. Chem.* **2005**, *26*, 1781–1802.
23. Humphrey, W.; Dalke, A.; Schulten, K. VMD: Visual Molecular Dynamics. *J. Mol. Graph.* **1996**, *14*, 33.
24. Shih, A. Y.; Freddolino, P. L.; Arkhipov, A.; Schulten, K. Assembly of Lipoprotein Particles Revealed by Coarse-Grained Molecular Dynamics Simulations. *J. Struct. Biol.* **2007**, *157*, 579–592.
25. O'Connell, M. J.; *et al.* Band Gap Fluorescence from Individual Single-Walled Carbon Nanotubes. *Science* **2002**, *297*, 593–596.
26. Moore, V. C.; Strano, M. S.; Haroz, E. H.; Hauge, R. H.; Smalley, R. E.; Schmidt, J.; Talmon, Y. Individually Suspended Single-Walled Carbon Nanotubes in Various Surfactants. *Nano Lett.* **2003**, *3*, 1379–1382.

27. Wu, Y.; Hudson, J. S.; Lu, Q.; Moore, J. M.; Mount, A. S.; Rao, A. M.; Alexov, E.; Ke, P. C. Coating Single-Walled Carbon Nanotubes with Phospholipids. *J. Phys. Chem. B* **2006**, *110*, 2475–2478.
28. Feller, S. E.; Zhang, Y. H.; Pastor, R. W.; Brooks, B. R. Constant-Pressure Molecular-Dynamics Simulation—The Langevin Piston Method. *J. Chem. Phys.* **1995**, *103*, 4613–4621.
29. Lantzsch, G.; Binder, H.; Heerklotz, H. Surface Area Per Molecule in Lipid/c12en Membranes As Seen by Fluorescence Resonance Energy Transfer. *J. Fluoresc.* **1994**, *4*, 339–343.
30. Liu, J.; Conboy, J. C. Kinetics and Thermodynamics of Association of a Phospholipid Derivative with Lipid Bilayers in Liquid-Disordered and Liquid-Ordered Phases. *Biophys. J.* **2005**, *89*, 2522–2532.
31. Abreu, M. S.; Moreno, M. J.; Vaz, W. L. Kinetics and Thermodynamics of Association of a Phospholipid Derivative with Lipid Bilayers in Liquid-Disordered and Liquid-Ordered Phases. *Biophys. J.* **2004**, *87*, 353–365.
32. Israelachvili, J. N.; Mitchell, D. J.; Ninham, B. W. Theory of Self-Assembly of Hydrocarbon Amphiphiles into Micelles and Bilayers. *J. Chem. Soc., Faraday Trans. 2* **1976**, *72*, 1525–1568.
33. Nagle, J. F.; Tristram-Nagle, S. Structure of Lipid Bilayers. *Biochim. Biophys. Acta* **2000**, *1469*, 159–195.
34. Doyle, D. A.; Cabral, J. M.; Pfuetzner, R. A.; Kuo, A. L.; Gulbis, J. M.; Cohen, S. L.; Chait, B. T.; MacKinnon, R. The Structure of the Potassium Channel: Molecular Basis of K^+ Conduction and Selectivity. *Science* **1998**, *280*, 69–77.
35. Ohvo-Rekila, H.; Ramstedt, B.; Leppimaki, P.; Slotte, J. P. Cholesterol Interactions with Phospholipids in Membranes. *Prog. Lipid Res.* **2002**, *41*, 66–97.
36. Palczewski, K.; *et al.* Crystal Structure of Rhodopsin: A G Protein-Coupled Receptor. *Science* **2000**, *289*, 739–745.
37. Peter, B. J.; Kent, H. M.; Mills, I. G.; Vallis, Y.; Butler, P. J. G.; Evans, P. R.; McMahon, H. T. BAR Domains As Sensors of Membrane Curvature: The Amphiphysin BAR Structure. *Science* **2004**, *303*, 495–499.
38. McMahon, H. T.; Gallop, J. L. Membrane Curvature and Mechanisms of Dynamic Cell Membrane Remodelling. *Nature* **2005**, *438*, 590–596.
39. Mohanty, N.; Berry, V. Graphene-Based Single-Bacterium Resolution Biodevice and DNA Transistor: Interfacing Graphene Derivatives with Nanoscale and Microscale Biocomponents. *Nano Lett.* **2008**, *8*, 4469–4476.
40. Shan, C.; Yang, H.; Song, J.; Han, D.; Ivaska, A.; Niu, L. Direct Electrochemistry of Glucose Oxidase and Biosensing for Glucose Based on Graphene. *Anal. Chem.* **2009**, *81*, 2378–2382.
41. Zhang, B.; Xing, Y.; Li, Z.; Zhou, H.; Mu, Q.; Yan, B. Functionalized Carbon Nanotubes Specifically Bind to α-Chymotrypsin's Catalytic Site and Regulate Its Enzymatic Function. *Nano Lett.* **2009**, *9*, 2280–2284.
42. Kim, K. S.; Zhao, Y.; Jang, H.; Lee, S. Y.; Kim, J. M.; Kim, K. S.; Ahn, J.-H.; Kim, P.; Choi, J.-Y.; Hong, B. H. Large-Scale Pattern Growth of Graphene Films for Stretchable Transparent Electrodes. *Nature* **2009**, *457*, 706–710.
43. Blakslee, O. L.; Proctor, D. G.; Seldin, E. J.; Spence, G. B.; Weng, T. Elastic Constants of Compression-Annealed Pyrolytic Graphite. *J. Appl. Phys.* **1970**, *41*, 3373–3382.
44. Frank, I. W.; Tanenbaum, D. M.; van der Zande, A. M.; McEuen, P. L. Mechanical Properties of Suspended Graphene Sheets. *J. Vac. Sci. Technol., B* **2007**, *25*, 2558–2561.
45. Lee, C.; Wei, X.; Kysar, J. W.; Hone, J. Measurement of the Elastic Properties and Intrinsic Strength of Monolayer Graphene. *Science* **2008**, *321*, 385–388.